

On the analysis of the temperature fluctuation in the Campi Flegrei caldera through a fractional Brownian motion-based model

A. Di Crescenzo⁽¹⁾, Barbara Martinucci^{(1)*}, and Verdiana Mustaro⁽¹⁾

(1) Dipartimento di Matematica, Università di Salerno
I-84084 Fisciano (SA), Italy Email: {adicrescenzo, bmartinucci, vmustaro}@unisa.it

April 9, 2024

Abstract

The aim of this research is to identify a model able to describe the fluctuations of the soil temperatures monitored in the volcanic caldera of the Campi Flegrei area in Naples (Italy). The study focuses on the data concerning the temperatures in the mentioned area through a seven-year period (cf. Sabbarese et al. [14]). The deterministic component of the model, given by the seasonal trend of the temperatures, is obtained through a regression method on the time series. A fractional Brownian motion (fBm) is chosen to represent the residual process between the seasonal trend and the time series. This is validated through a suitable test and an estimation based on the periodogram of the data. Thereafter, the Hurst exponent of the process is estimated by means of a method proposed by Cannon et al. [2]. Finally, an inference test based on the detrended moving average of the data is adopted in order to confirm that the residual series follows a fBm.

Keywords: Fractional Brownian motion, Hurst exponent, Campi Flegrei caldera, temperature fluctuation

1 Introduction

In several application contexts, one of the main problems in the description of a phenomenon that evolves over time is the individuation of the probabilistic laws by which the phenomenon itself is driven. To this aim, schemes based on the superimposition of deterministic and random components are often chosen, in which the deterministic part describes the phenomenon's trend, while the random one describes the fluctuations determined by unpredictable exogenous factors. An example of such model is presented in the work by Sebastiani and Malagnini [15], where a physical model with

*Corresponding author

non-constant variance is proposed to describe the phenomenon of coupling erosion that caused the 2011 earthquake in Tohoku-Oki (Japan).

The aim of this study is to implement an analogous scheme to describe the soil temperatures observed on the surface of the Campi Flegrei caldera. This volcanic area is located near the city of Naples, in Italy, and is famous for the ground deformations that have been registered in the area since ancient times. Recent observations, carried out in the years from 2011 to 2017, were led to monitor the presence of radon in two sites of the area (cf. Sabbarese et al. [14]). In the work [14], the presence of radon in the soil was tracked, along with its dependence on physical quantities such as temperature, pressure and humidity, in order to prove how the seismic activity in the Campi Flegrei area was influenced by the presence of the element.

Starting from the research mentioned above, in this work we aim to build a model able to describe the fluctuations of soil temperatures in the caldera through the identification of the temporal trend and the corresponding random component.

What emerged from the present study is that the deterministic component is well described by a piecewise linear model. In this model, the segments' slopes are alternating in sign and can be determined by conducting a linear regression on the observed data. The stochastic model individuating the random fluctuations component is instead recognized to be the fractional Brownian motion (fBm). For a description of the most relevant probabilistic aspects of fBm see, for example, Nourdin [11]. This stochastic process has been proposed in several studies for modeling various geophysical phenomena. In the work by Mattia et al. [8], fBm is proposed as an approximation of the process describing the trend of ground data involving soil roughness collected over three different European sites. In the paper by Yin and Ranalli [20], the authors show that the event of earthquake rupturing in a fault is related to factors such as static shear stress and static frictional strength through the potential dynamic stress drop. The latter is regarded as a one-dimensional stochastic process and it is modeled as a fractional Brownian motion with Hurst exponent close to zero.

The evidence of reasonableness of the model firstly emerges as consequence of a statistical test, in which the hypothesis that the random fluctuations of the model can be described by a Brownian motion is rejected. The subsequent phase of the work involves the study of the periodogram of the data, and allows to verify that the random fluctuations are well described by a fBm, in opposition to a fractional Gaussian noise (fGn). Part of the study was also devoted to the estimation of the parameters involved, namely the Hurst exponent and the scale parameter of the fBm. Many estimation techniques for the former parameter have been proposed in the literature. Several methods are presented in [17], and other works often provide modified versions of the already known algorithms, see, for instance, [10]. For the estimation of the Hurst exponent we used a method proposed by Cannon et al. in [2], which is based on the evaluation of the arithmetical average of the standard deviations of the data, obtained by collecting them in sequential windows, repeating the operation for different increasing choices of the windows' size. The goodness of the model involving the fBm process has finally been confirmed through an hypothesis testing in which the test statistic involved the detrending moving averages obtained from the data.

Here is the plan of the article. In Section 2 we introduce the starting equation modeling the soil temperatures trend (cf. (1)) and we describe the main features of fBm.

Section 3 focuses on the data analysis directed towards identifying the deterministic component of the temperatures trend. A statistical test that allows to reject the hypothesis of the random component being a Brownian motion is also conducted. The remaining part of the article is dedicated to the analysis of the stochastic component of the model. More specifically, Section 4 is aimed to the study of the periodogram obtained from the data observations, from which emerges the eligibility of fBm to describe the random component of the temperature compared to fGn. In Section 5 we conduct an estimation of the relevant parameters of the process, i.e. the Hurst exponent and the scale parameter. The work is completed by Section 6, which contains the statistical test leading to the acceptance of the model based on fBm, and Section 7, which collects the conclusions of the study.

2 The stochastic model

The time series considered throughout this study describes the temperatures of the surface soil of the Campi Flegrei caldera, obtained via daily observations in the time period between 07/01/2011 and 12/31/2017. The main aim of the research is to develop a model able to describe the fluctuations of the data. As usually observed in geophysical studies, the trajectory of the time series is seen as the superposition of a deterministic component and a stochastic one, where the latter represents the fluctuations from the trend. As a consequence, the process $\{X(t), t \geq 0\}$ that represents the daily observed soil temperatures is described by the equation

$$X(t) = r(t) + B_H(t), \quad (1)$$

where $r(t)$ constitutes the deterministic component of the process, while $B_H(t)$ is a stochastic process. We will show that a suitable assumption is to identify $B_H(t)$ a fBm. A similar model has been proposed for the vertical motion of the soil in the Campi Flegrei area, cf. Travaglino et al. [18].

Under the assumption that $B_H(t)$ is indeed a fBm, it is easy to observe that the model shown in (1) is such that $\mathbb{E}(X(t)) = r(t)$. We recall, in fact, that the fractional Brownian motion is a continuous-time Gaussian process with zero mean and covariance

$$\text{Cov}[B_H(t), B_H(s)] = D(t^{2H} + s^{2H} - |t - s|^{2H}), \quad t, s \geq 0, \quad (2)$$

where $D > 0$ is a scale parameter, named diffusion constant, and $0 < H < 1$ is a parameter known as the Hurst exponent. The process was first introduced by Mandelbrot and Van Ness in [7]. It is a generalization of the Brownian motion, since for $D = 1/2$ and $H = 1/2$ it reduces to a standard Wiener process. We remark that fBm has the property of self-similarity, that is, for any choice of $a > 0$,

$$\{B_H(at), t \geq 0\} \stackrel{d}{=} \{a^H B_H(t), t \geq 0\},$$

meaning that the two processes are equal in distribution. The parameter H is therefore also referred to as the scaling exponent or fractal index of the process.

The model (1) is not stationary, since fBm is not a stationary process itself. The process of the increments of $B_H(t)$, defined by $Z(t) = B_H(t+1) - B_H(t)$ for all $t \geq 0$, is however stationary. This is known as fractionary Gaussian noise (fGn).

Introducing the process $Z(t)$ leads to another well-known property of fBm, that is the long-range dependency (LRD). As pointed out in [3], a stationary process $X(t)$ has long-range dependence (or is a long memory process) if its autocorrelation function, defined as

$$\rho(k) = \frac{\text{Cov}(X(t), X(t+k))}{\text{Var}[X(1)]},$$

satisfies the condition

$$\sum_{k=-\infty}^{+\infty} \rho(k) = \infty.$$

This definition implies that the autocorrelation of the process decays slowly over time, making the sum of the autocorrelations divergent; therefore, if $X(t)$ is a LRD process, then

$$\lim_{k \rightarrow +\infty} \frac{\rho(k)}{ck^{-\alpha}} = 1, \quad (3)$$

where $c > 0$ and $0 < \alpha < 1$ are constants. This definition states that the decay of the autocorrelation function is power-like, hence slower than exponential. In the case of fBm, long-range dependence can be seen looking at the increments in $Z(t)$. Moreover, the parameter α is related to the Hurst exponent through the equation $\alpha = 2H - 2$, evidencing that the value of the Hurst exponent can be used to determine the nature of the process. We recall that (see also [3] and [6])

- if $\frac{1}{2} < H < 1$, then the increments of the process are positively correlated, making the process persistent, i.e. likely to keep the trend exhibited in the previous observations;
- if $0 < H < \frac{1}{2}$, the increments of the process are negatively correlated and the process is counter-persistent, i.e. likely to break the trend followed in the past.

A relation similar to (3), but concerning the frequency domain of the time series, is shown in Section 3, where it is used for the estimation of a parameter of the process.

3 Data analysis

The model (1) is used to analyze the time series regarding the temperatures of the Campi Flegrei caldera soil, cf. Sabbarese et al. [14]. The initial data set is consisting of $N + 1 = 2005$ observations, collected in the times indicated by t_0, t_1, \dots, t_N and shown in the scatter plot in Figure 1. A seasonal trend is clearly visible in the dataset, with the temperatures increasing during spring and summer in each year of observation, and then starting to decrease around September. For this reason, the trend $r(t)$ is constructed by alternating segments with opposite slopes, obtained from the data

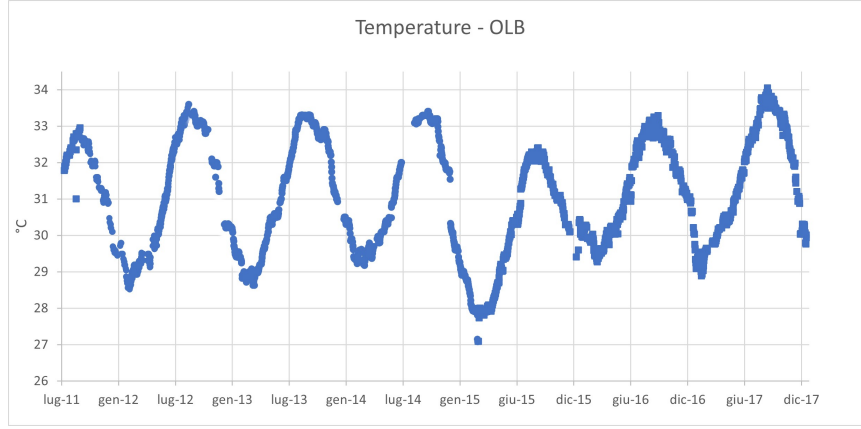


Figure 1: Scatter plot of the data series $X(t)$ for the temperatures of the surface soil of the Campi Flegrei caldera in the Monte Olevano (NA) site.

Table 1: Local maxima and minima for each section of the dataset and the corresponding dates (mm/dd/year).

| τ_i | $\max(X(\tau_i))$ (°C) | τ_i | $\min(X(\tau_i))$ (°C) |
|------------|------------------------|------------|------------------------|
| 07/29/2011 | 31.78 | 02/12/2012 | 28.68 |
| 08/25/2012 | 33.6 | 03/22/2013 | 28.63 |
| 09/11/2013 | 33.31 | 03/04/2014 | 29.17 |
| 09/22/2014 | 33.4 | 02/27/2015 | 27.08 |
| 09/05/2015 | 32.4 | 03/11/2016 | 29.27 |
| 09/19/2016 | 33.29 | 02/03/2017 | 28.88 |
| 08/30/2017 | 34.04 | | |

through linear regression. To this aim, the dataset is divided into 15 sections. The first and the last measurements are given by

$$\begin{aligned}\tau_0 &= 07/29/2011, & X(\tau_0) &= 31.78; \\ \tau_N &= 12/31/2017, & X(\tau_N) &= 29.94.\end{aligned}$$

These points, together with 13 local minima and maxima, are used as the extreme points of the sections. In order to obtain a piecewise linear curve, for each couple of consecutive equations, we consider the constraints

$$m_i + q_i \tau_i = m_{i+1} + q_{i+1} \tau_{i+1}, \quad i = 1, 2, \dots, 14,$$

where τ_i and τ_{i+1} represent two consecutive extremes of the intervals, as collected in Table 1.

Writing these equations for each couple of linear polynomials, a system of constraints has been obtained, from which the parameters are calculated. The missing pa-

Table 2: Slopes obtained for the piecewise linear polynomial approximating the data series, and the corresponding coefficients of determination R^2 .

| i | c_i | R^2 | v_i | R^2 |
|-----|--------|--------|---------|--------|
| 1 | 0.0193 | 0.9442 | -0.0284 | 0.9690 |
| 2 | 0.0271 | 0.9401 | -0.0280 | 0.9679 |
| 3 | 0.0291 | 0.9831 | -0.0268 | 0.9572 |
| 4 | 0.0234 | 0.9703 | -0.0421 | 0.9625 |
| 5 | 0.0293 | 0.9687 | -0.0143 | 0.9150 |
| 6 | 0.0226 | 0.9595 | -0.0285 | 0.9275 |
| 7 | 0.0237 | 0.9676 | -0.0344 | 0.9064 |

parameters for the regression lines are estimated using the ordinary least squares (OLS) method. The operation is repeated in each interval delimited by the values in Table 1.

The alternating slopes $c_i > 0$ and $v_i < 0$ obtained for the regression model are reported in Table 2, together with the coefficient of determination R^2 for each line. The values obtained are used to identify the deterministic component $r(t)$ of the model (1). The values of R^2 confirm that the regression lines provide a good fitting of the data in each interval. The resulting linear model is shown with the scatter plot in Figure 2.

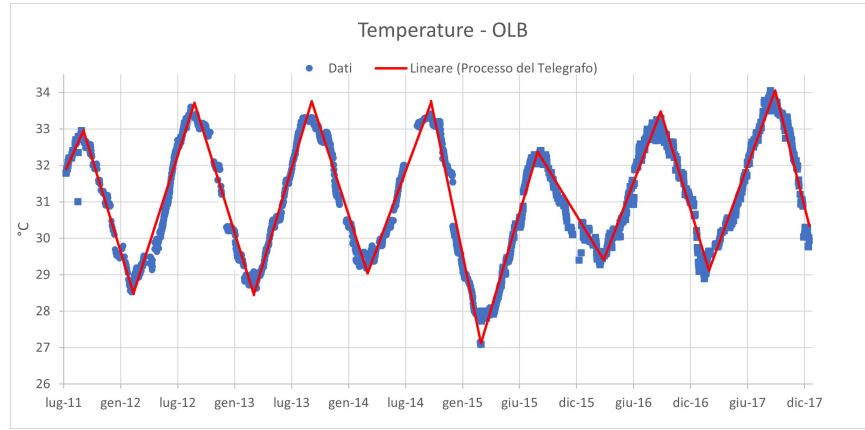


Figure 2: Scatter plot of the data series $X(t)$ and linear approximation of the deterministic trend $r(t)$.

3.1 Testing for Brownian motion

The residuals concerning the least squares lines are shown in Figure 3. With reference to (1), aiming to assess the suitable nature of the process $B_H(t)$, hereafter we show that the assumption of $B_H(t)$ being a Brownian motion ($B(t)$) cannot be accepted. The

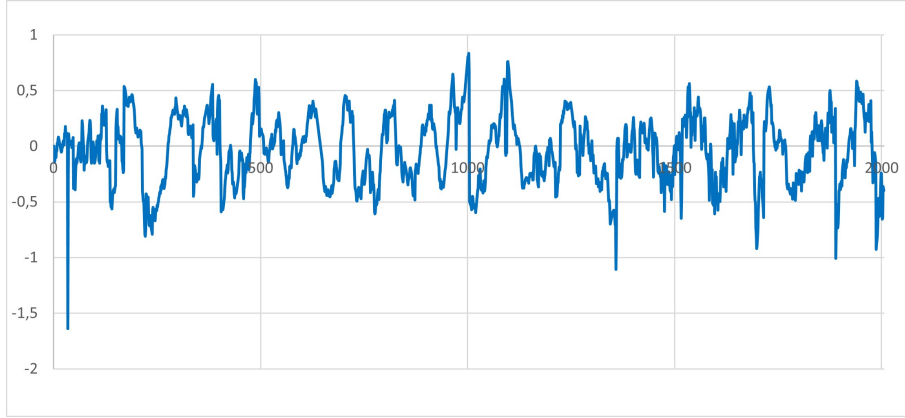


Figure 3: Residual series $B_H(t) = X(t) - r(t)$.

statistical test implemented to this aim is the one proposed by Briane et al. in [1]. The hypothesis of the test are

$$\begin{aligned}\mathcal{H}_0 : B_H(t) &= \sigma B(t), \\ \mathcal{H}_1 : B_H(t) &\text{ is a confined or directed diffusion.}\end{aligned}$$

The asymptotic region of acceptance for \mathcal{H}_0 is given by

$$\left\{ q\left(\frac{\alpha}{2}\right) \leq \frac{S_D^N}{\hat{\sigma}\sqrt{t_N}} \leq q\left(1 - \frac{\alpha}{2}\right) \right\},$$

where

$$\begin{aligned}S_D^N &= \max_{j=1, \dots, N} |B_H(t_j) - B_H(t_0)|, \\ \hat{\sigma} &= \left\{ \frac{1}{N} \sum_{j=1}^N \frac{[B_H(t_j) - B_H(t_{j-1})]^2}{t_j - t_{j-1}} \right\}^{1/2},\end{aligned}$$

and $q(\alpha)$ is the quantile of

$$\sup_{0 \leq s \leq 1} |B(s) - B(0)|,$$

where $B(t)$ is the Brownian process.

The extremes of the acceptance interval for the significance level $\alpha = 0.05$ are given by

$$q(0.025) = 0.834, \quad q(0.975) = 2.940,$$

while the value obtained for the test statistic is 0.087. The null hypothesis of the process being a Brownian motion is therefore rejected. This justifies the further analysis conducted hereafter.

4 Analysis of the stochastic component

In this section we aim to investigate whether the time series of the residuals represents a fractional Brownian motion or a fractional Gaussian noise. We recall that such two processes, due to their nature, require different estimation procedures.

Before proceeding, we perform some preparatory operations on the dataset. Since the initial series is not equally spaced, as the measurements for temperature in some days are missing, we collect the missing data by performing a linear interpolation, covering the whole observation period. The outliers are also detected and removed through a box-plot of the residuals. The prepared dataset obtained after this phase consists of $N + 1 = 2346$ observations.

We subsequently evaluate the Fourier spectrum $S(f)$ of the data, plotting it against the frequencies f on a log-log scale. This is done using the periodogram of the data series, which is computed using the modified periodogram method suggested by Welch in [19]. The technique consists in dividing the signal into overlapping segments and averaging the modified periodograms calculated in each window to obtain the final result. The data has also been modified with an adjustment proposed in [5], called end-matching, which consists in subtracting to the data, in each window, the corresponding values of the line through the first and last point of the segment. This makes the estimation of the spectral density function more reliable. The Welch's modified periodogram is shown in Figure 4.

A relation analogous to (3) for long memory processes can be also presented in the frequency domain of the time series. In this context, the estimated Fourier spectrum $S(f)$ and the frequencies f are asymptotically evaluated as

$$S(f) = S(f_0) \cdot f^{-\beta}, \quad (4)$$

where both $S(f_0)$ and β are constants. The coefficient β is linked to the Hurst exponent H by different equations, depending on the process. Indeed,

$$\begin{aligned} \text{if } B_H(t) \text{ is a fGn, then } \beta &= 2H - 1, \\ \text{if } B_H(t) \text{ is a fBm then } \beta &= 2H + 1, \end{aligned}$$

cf. [13], [9] and [4]. Recalling that $0 < H < 1$ always holds, if $-1 < \beta < 1$, then the time series can be identified as a realization of a fractional Gaussian noise, while if $1 < \beta < 3$ it can be concluded that the data represent a sample path of a fractional Brownian motion. From (4) we get

$$\log S(f) = \log S(f_0) - \beta \log f.$$

Therefore, we obtain an estimation for the coefficient β by plotting on a log-log scale the frequencies and the values for $S(f)$ attained through the periodogram and then taking the opposite value of the slope of the least squares line as estimation. The results are shown in Figure 5 both for raw data and data treated with the end-matching technique. The β values obtained via the slopes of the regression lines and the R^2 values are reported in Table 3. It is shown that the resulting values are similar and the coefficients of determination are consistently high, meaning that in our case the use of end-matching is not essential for the estimation of the parameter.

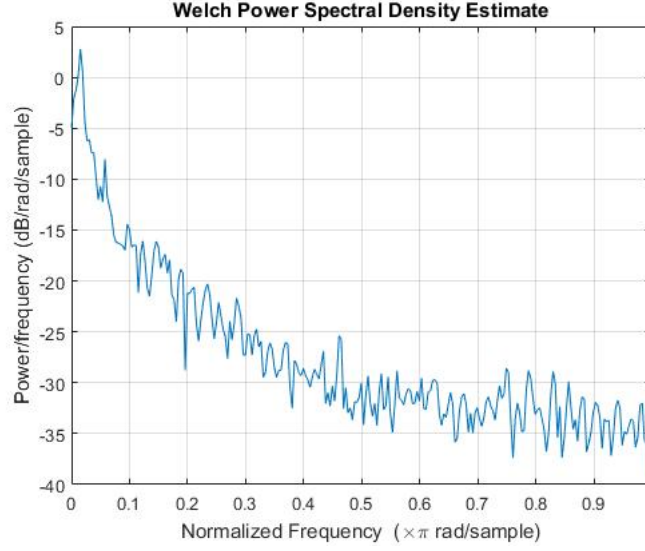


Figure 4: Modified Welch periodogram for the data series $B_H(t)$, plotted for different values of the frequency.

Table 3: Values of β and relative coefficients of determination obtained from the series of the residuals $B_H(t)$ using Welch's modified periodogram.

| | Welch's periodogram | Welch's periodogram (with end-matching) |
|---------|---------------------|--|
| β | 1.831 | 1.844 |
| R^2 | 0.925 | 0.929 |

In both cases, the coefficient β belongs to the interval $(1, 3)$, and therefore we can conclude that the data series follows a fBm trend.

5 Parameter estimation

Once established that the time series can be seen as a sample path of fBm, hereafter we obtain an estimation of the parameters of such a process. To this aim, we use the scaled windowed variance method from Cannon [2] to find an estimation for the Hurst exponent H .

The method requires first that the dataset is divided into non-overlapping windows, each of fixed length n , chosen among the powers of 2. By doing so, k windows are obtained from the available dataset, with $kn \leq N + 1$. Before proceeding, we apply a process of trend removal, as suggested in Cannon [2], removing from the data the

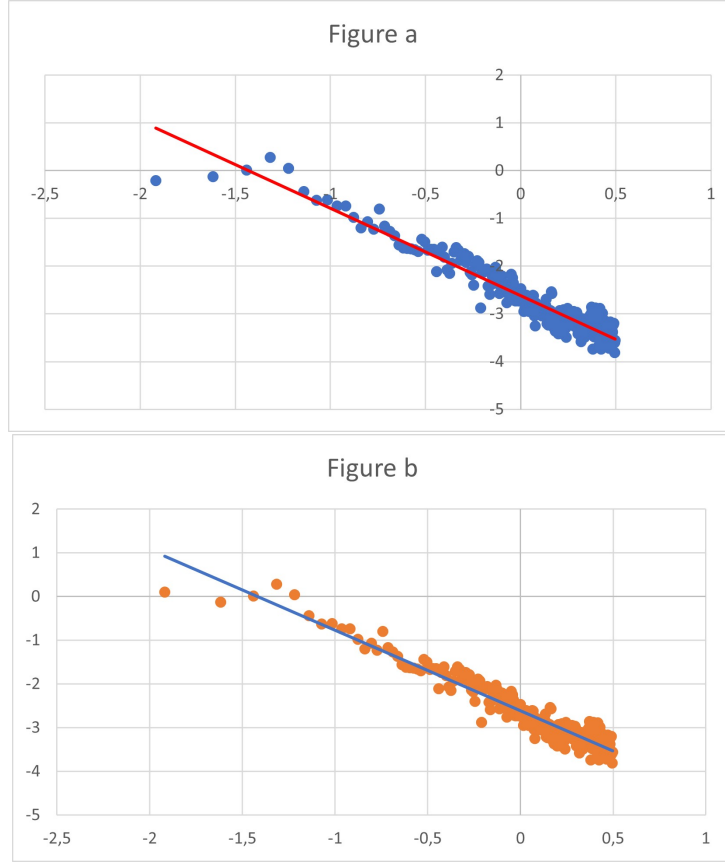


Figure 5: Log-log plot for the Welch's periodogram of the data series against frequency, obtained by using both raw data (a) and treating data with end-matching (b). The slope of the least squares line estimates the coefficient β .

line between the first and the last observation of each window (bridge detrended scaled windowed variance). The standard deviation is then calculated in each window, thus getting

$$SD_i(n) = \frac{1}{n-1} \sqrt{\sum_{j=0}^{n-1} (B_H(t_{(i-1)n+j}) - \bar{B}_{H,i})^2}, \quad i = 1, 2, \dots, k,$$

where $\bar{B}_{H,i}$ is the average of the data in the i -th window and the $B_H(t_{(i-1)n+j})$ are the values in such window. The average of the standard deviations $SD_i(n)$ is then calculated and denoted by $\overline{SD}(n)$. The procedure is then repeated for $n = 1, 2, 4, \dots, 2^k$, where 2^k is the highest power of 2 such that $2^k \leq N + 1$. Subsequently, the values of $\overline{SD}(n)$ are plotted against n on a log-log plot, see Figure 6. The estimate for H is obtained as the slope of the minimum squares regression line, considered on a reduced number of

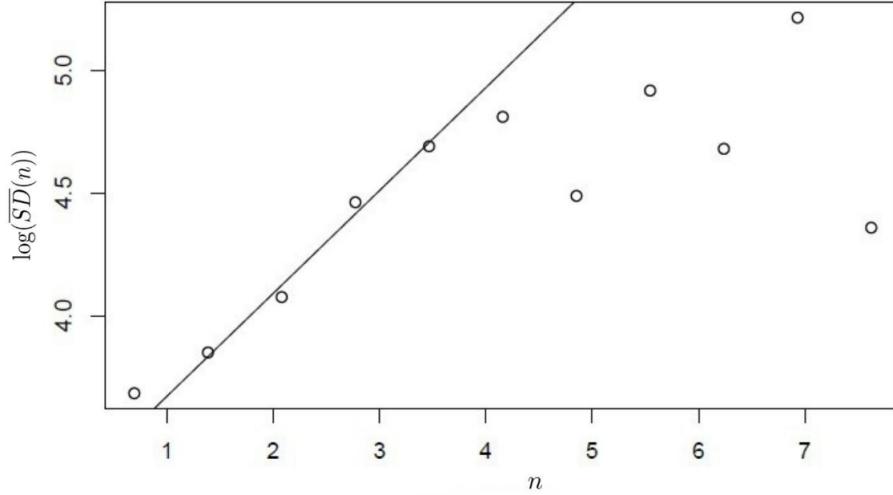


Figure 6: Log-log plot of the averaged standard deviations obtained with the scaled windowed variance method against the length n of the windows used.

points. In fact, as mentioned in [2], some of the highest and lowest values of n need to be excluded. This is mainly due to the fact that, for low values of n , the windows are too small to give an accurate evaluation of $SD_i(n)$, while for high values of n the number of windows is not enough to obtain a reliable average value. The number of cases to exclude varies depending on the size of the data series and the type of trend removal. In our case, the considered values range between $n = 2^2$ and $n = 2^5$, cf. Figure 6. The estimate obtained for the Hurst index is

$$\hat{H} = 0.4562.$$

With reference to the obtained estimate for H , the process $B_H(t)$ is seen as a fBm with negatively correlated increments.

The last part of the estimation phase consists in the evaluation of the diffusion constant D , which is done directly from the data, calculating the sample variance of the increments $B_H(t) - B_H(t-1)$ of the data series. The estimate obtained so far is

$$\hat{D} = 0.0846.$$

6 Statistical test for the model

To further confirm the results obtained in Section 5, we perform a statistical test on the data series for the hypothesis of $B_H(t)$ being a fractional Brownian motion with parameters $\hat{H} = 0.4562$ and $\hat{D} = 0.0846$. To this aim, we use the inference test presented in Sikora [16], based on the detrending moving average of the data, therefore called DMA statistic test. The null hypothesis for the test is

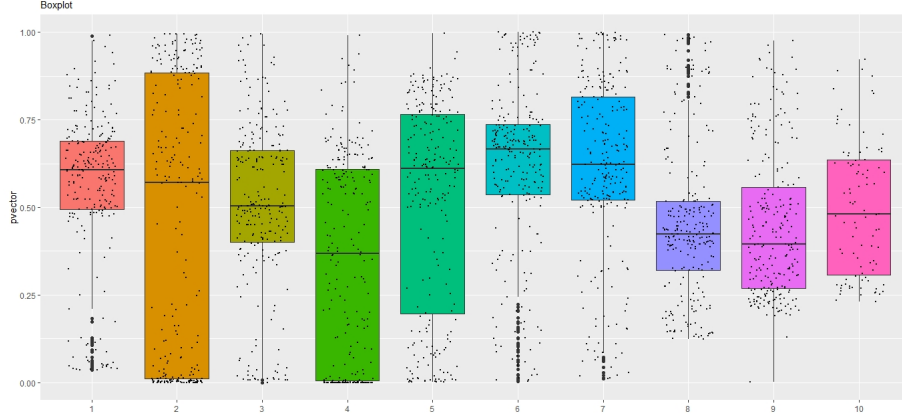


Figure 7: Box plot for the values of p obtained in the 10 subsets of the data.

$\mathcal{H}_0 : \{B_H(t_1), B_H(t_2), \dots, B_H(t_N)\}$ is a trajectory of fBm with parameters \hat{H} and \hat{D} , while the alternative hypothesis is

$\mathcal{H}_1 : \{B_H(t_1), B_H(t_2), \dots, B_H(t_N)\}$ is not a trajectory of fBm with parameters \hat{H} and \hat{D} .

The corresponding test statistic, for fixed $m > 1$, is given by

$$\sigma^2(m) = \frac{1}{N-m} \sum_{j=m}^N (B_H(t_j) - \bar{B}_H^m(t_j))^2 := \xi, \quad (5)$$

where $\bar{B}_H^m(t_j)$ denotes the moving average of the previous m observations $\{B_H(t_{j-i}), i = 0, 1, \dots, m-1\}$.

The p -value for this test is defined by an infinite series, so it needs to be computed as an empirical quantile, obtained from series of generalized chi-squared random variables. Recalling Step 5 in Section 3 of Sikora [16], the p -value of the test is calculated as

$$p = \frac{2}{L} \min\{\#(\sigma_l^2(m) < \xi), \#(\sigma_l^2(m) > \xi)\}. \quad (6)$$

In this formula, L is the number of samples generated for the chi-squared distribution. For a good estimate of p we set $L = 1000$. Moreover, in Eq. (6), we consider

$$\sigma_l^2(m) = \frac{1}{N-m} \sum_{j=1}^{N-m+1} \lambda_j(m) U_j^l, \quad l = 1, 2, \dots, L,$$

where $\mathbf{U}^l = \{U_1^l, U_2^l, \dots, U_{N-m+1}^l\}$ is the l -th chi-square sample and $\lambda_j(m)$ is the j -th eigenvalue of the sample matrix

$$\tilde{\Sigma} = \{\mathbb{E}[B_H(t_j)B_H(t_k)], j, k = 1, 2, \dots, N-m+1\}.$$

Table 4: Number of cases in which the DMA statistic test has different outcomes for the data series $B(t)$.

| Set | Reject values ($p \leq 0.02$) | Perc. | Warning values ($0.02 \leq p \leq 0.05$) | Perc. | Acceptable values ($p > 0.05$) | Perc. |
|-----|------------------------------------|--------|---|-------|-------------------------------------|--------|
| 1 | 0 | 0% | 12 | 4.86% | 235 | 95.14% |
| 2 | 70 | 28.23% | 12 | 4.84% | 154 | 62.10% |
| 3 | 17 | 6.85% | 6 | 2.42% | 219 | 88.31% |
| 4 | 70 | 28.23% | 6 | 2.42% | 166 | 66.94% |
| 5 | 23 | 9.27% | 10 | 4.03% | 205 | 82.66% |
| 6 | 4 | 1.61% | 4 | 1.61% | 236 | 95.16% |
| 7 | 3 | 1.21% | 3 | 1.21% | 239 | 96.37% |
| 8 | 0 | 0% | 0 | 0% | 248 | 100% |
| 9 | 1 | 0.4% | 0 | 0% | 247 | 99.6% |
| 10 | 0 | 0% | 0 | 0% | 95 | 100% |

Recalling (5), since the search for an optimal value for m is still an open question, we divide the data series into 10 subsets of about 250 observations each, in order to adapt the procedure even to cases with large number of observed data. Then we run the test in every subset for each suitable value of m .

After, we collect the p -values and create a box plot with jitter for each subset, in order to determine the outlier values for p , cf. Figure 7.

The significance level considered for this test is $\alpha = 0.02$, therefore the results in each subset are collected and divided into three categories:

- (i) for $p \leq 0.02$, the null hypothesis is rejected,
- (ii) for $0.02 < p \leq 0.05$ the values are considered as "warning",
- (iii) for $p > 0.05$ the hypothesis \mathcal{H}_0 cannot be rejected.

The results are shown in Table 4. A percentage of the number of rejected, warning and acceptable values over the total of p -values calculated in the 10 datasets is also included. It can be observed that the hypothesis of $B_H(t)$ being a fBm with the coefficients estimated in the previous phase cannot be rejected in almost 90% of the cases covered, considering all the subsets in which the data were divided and all the different choices of n for the test statistic. This allows to affirm the validity of the hypothesis that the time series of the residuals follows a fBm trend.

7 Conclusions

The research conducted shows that the stochastic model proposed for the data is well-fitting of the empirical time series of the temperatures. It can be seen from the results obtained in the phases of data analysis and parameter estimation that the coefficients obtained to describe the process $X(t)$ designed in the beginning always display high values for the coefficient of determination R^2 , which is monitoring the goodness of the fit given by the model designed for the data. In summation, the study revealed that

the motion of the temperatures in the Campi Flegrei caldera is correctly modeled by a deterministic component, that clearly represents the seasonal trend, and a fractional Brownian motion as the process of residuals.

Acknowledgements

The authors are members of the research group GNCS of INdAM (Istituto Nazionale di Alta Matematica).

This work is supported in part by the Italian MIUR-PRIN 2017, project ‘Stochastic Models for Complex Systems’, No. 2017JFFHSH.

References

- [1] V. Briane *et al.* (2016), *An adaptive statistical test to detect non Brownian diffusion from particle trajectories*. ISBI 2016-IEEE 13th Symposium on Biomedical Imaging.
- [2] M. Cannon, D. Percival, D. Caccia *et al.* (1997), *Evaluating scaled windowed variance methods for estimating the Hurst coefficient of time series*. Physica A: Statistical Mechanics and its Applications, Volume 241, Issues 3–4, Pages 606-626, ISSN 0378-4371.
- [3] T. Dieker, (2004). *Simulation of Fractional Brownian Motion*. Ph.D. Thesis, 160 Physics Department of Mathematical Sciences, University of Twente.
- [4] P. Flandrin, (1989). *On the spectrum of fractional Brownian motions*. IEEE Transactions on Information Theory, vol. 35, no. 1, pp. 197-199, Jan. 1989, doi: 10.1109/18.42195.
- [5] P. Fougere (1985), *On the accuracy of spectrum analysis of red noise processes using maximum entropy and periodogram methods: Simulation studies and application to geophysical data*. Journal of Geophysical Research 90, 4355-4366.
- [6] M. Li (2013), *On the Long-Range Dependence of Fractional Brownian Motion*. Mathematical Problems in Engineering. 2013. 10.1155/2013/842197.
- [7] B. B. Mandelbrot, J. W. Van Ness (1968), *Fractional Brownian Motions, Fractional Noises and Applications*. SIAM Review, vol. 10, no. 4, 1968, pp. 422–437.
- [8] F. Mattia, T. Le Toan, M. Davidson, M. Borgeaud (1999), *On the scattering from natural rough surfaces*. 2413 - 2415 vol.5. 10.1109/IGARSS.1999.771527.
- [9] A. Montanari, M.S. Taqqu, V. Teverovsky (1999). *Estimating Long-Range Dependence in the Presence of Periodicity: An Empirical Study*. Mathematical and Computer Modelling. 29. 217-228. 10.1016/S0895-7177(99)00104-1.
- [10] J. Montillet, K. Yu (2011), *Leaky LMS Algorithm and Fractional Brownian Motion Model for GNSS Receiver Position Estimation*, 2011 IEEE Vehicular Technology Conference (VTC Fall), pp. 1-5, doi: 10.1109/VETECF.2011.6092850.

- [11] I. Nourdin (2012). *Selected Aspects of Fractional Brownian Motion*. Springer. 4, 2012, Bocconi & Springer Series. (hal-01314412)
- [12] B. L. S. Prakasa Rao (2010). *Statistical Inference for Fractional Diffusion Processes*. 10.1002/9780470667125.
- [13] C. Roume, S. Ezzina, H. Blain, D Delignieres (2019). *Biases in the Simulation and Analysis of Fractal Processes*. Computational and Mathematical Methods in Medicine. 2019. 1-12. 10.1155/2019/4025305.
- [14] C. Sabbarese, F. Ambrosino, G. Chiodini *et al.* (2020), *Continuous radon monitoring during seven years of volcanic unrest at Campi Flegrei caldera (Italy)*. Scientific Reports 10:9551;
- [15] G. Sebastiani, L. Malagnini (2020). *Forecasting the Next Parkfield Mainshock on the San Andreas Fault (California)*. Journal of Ecology & Natural Resources. 4. 10.23880/JENR-16000218.
- [16] G. Sikora (2018), *Statistical test for fractional Brownian motion based on detrending moving average algorithm*. Chaos, Solitons & Fractals, Volume 116, 54-62, ISSN 0960-0779;
- [17] M. S. Taqqu, V. Teverovsky, W. Willinger (1996), *Estimators for longrange dependence: an empirical study*. Fractals, vol. 3, no. 4, pp. 785- 798, 1995. Reprinted in C.J.G. Evertsz, H.-O. Peitgen, R.F. Voss (Eds.), Fractal Geometry and Analysis, World Scientific, Singapore.
- [18] F. Travaglino, A. Di Crescenzo, B. Martinucci, R. Scarpa (2018), *A New Model of Campi Flegrei Inflation and Deflation Episodes based on Brownian Motion Driven by Telegraph Process*. Mathematical Geosciences (2018) 50:961-975;
- [19] P. Welch (1967), *The use of fast Fourier transform for the estimation of power spectra: A method based on time averaging over short, modified periodograms*. IEEE Transactions on Audio and Electroacoustics, vol. 15, no. 2, pp. 70-73, doi: 10.1109/TAU.1967.1161901.
- [20] Z.M. Yin, G. Ranalli (1995) *Modelling of earthquake rupturing as a stochastic process and estimation of its distribution function from earthquake observations*. Geophysical Journal International, Volume 123, Issue 3, pp. 838–848.